Indian J. pure appl. Math., 34(1) : 31-47, January 2003

APPLICATION OF NATURAL GENERALISED INVERSE TECHNIQUE IN RECONSTRUCTION OF GRAVITY ANOMALIES DUE TO A FAULT

M. M. MALLESWARA RAO*, T. V. RAMANA MURTY*, K. S. R. MURTHY* AND R. Y. VASUDEVA**

*National Institute of Oceanography, Regional Center, 176, Lawsons Bay, Visakhapatnam, India

**Department of Applied Mathematics, Andhra University, Visakhapatnam, India

(*Received* 25 *September* 2000; *after revision* 5 *February* 2002; *accepted* 6 *May* 2002)

Generalised Inverse (GI) and Singular Value Decomposition (SVD) are well known mathematical techniques exploited in many areas of applied science including the earth sciences. Simulation experiments on gravity anomaly due to a subsurface fault model have been carried out in the present work to estimate accurate model parameters by inverting the observed anomaly using GI approach via SVD.

While solving the inverse problem, data kernel has been generated through the model. Using this data kernel, SVD has been performed to build Generalised Inverse Operator (GIO) and it is operated on the observed anomaly with reference to the calculated anomaly to update model parameters. Data and model resolution matrices are computed to check the correctness of the solution.

A gravity profile over the Garber Oil Field, Oklahoma, equating to a fault has been studied to test/validate the procedure. The obtained values of the optimized model parameters of the oil field tally with the published results. Analysis reveals that among all the parameters density contrast and datum level dominates the energy modes of the data and model space over 99.3% while the remaining make negligible contribution. The merits of SVD are illustratively discussed.

Key Words : Gravity Anomaly; Fault; Inverse; Data Resolution; Model Resolution

1. INTRODUCTION

Geophysical methods are based on the application of certain physical principles to study the geological problems of the earth's interior. Mathematical techniques are employed with profit in all these applications.

Gravity and Magnetic methods are routinely used in exploration geophysics to locate the geological structures favourable for mineral and oil occurrences. The method in essence comprises collection, processing and interpretation of data in terms of a viable geological model. The estimation of the model parameters of the causative sources that are responsible for the observed anomalies forms part of data interpretation. Exploring reliable mathematical tools for the estimation of the causative source parameters is the concern of the present article.

Interpretation techniques of gravity and magnetic data generally employ indirect methods for translating the observed gravity or magnetic anomalies (Fig. 1) into sub-surface geology. The general procedure is to assume appropriate geometry for the causative source and compute its gravity effect and modify the model progressively until a reasonable fit with the observed anomaly is obtained

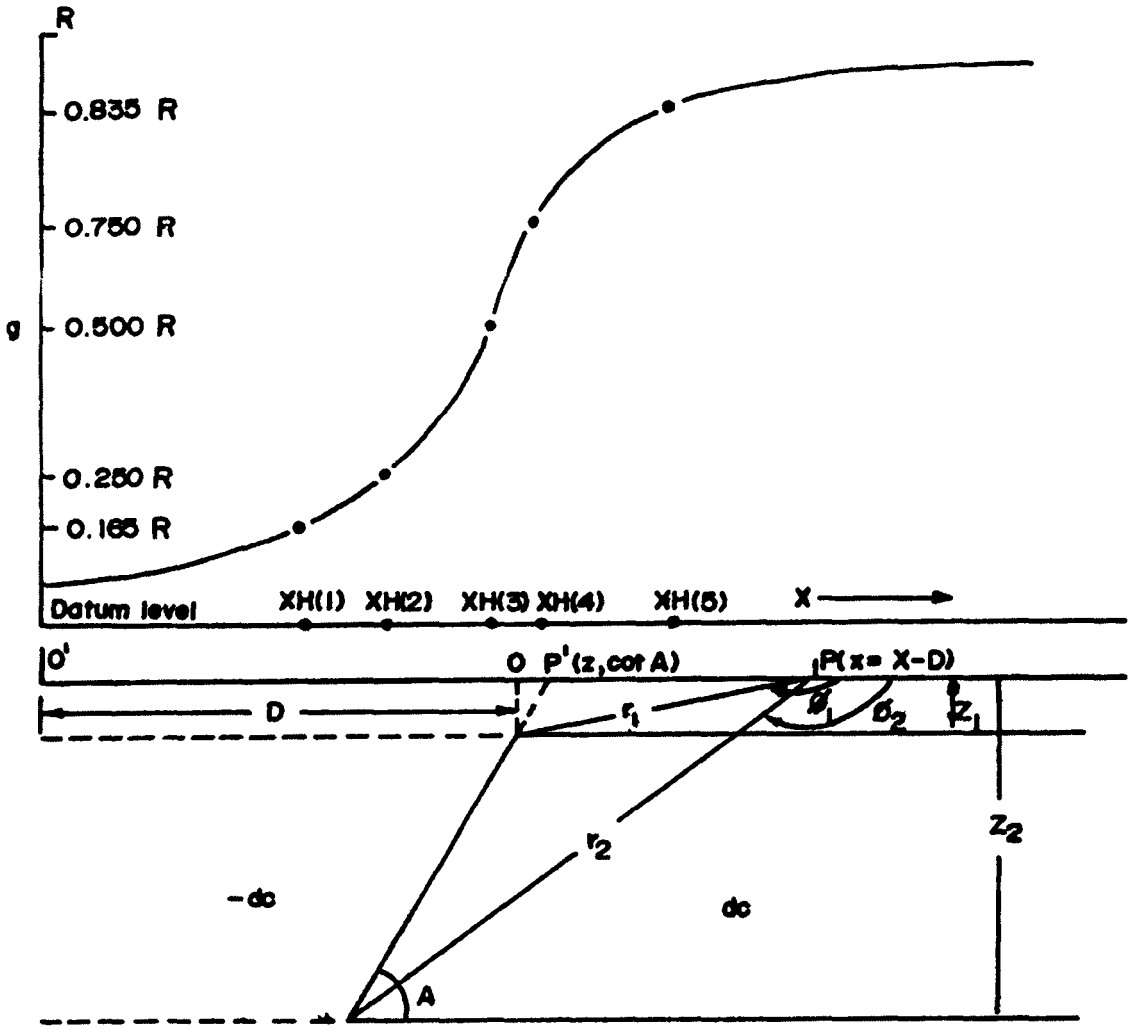

FIG. 1. Gravity anomaly and parameters of fault model

(Talwani and Heirtzler[26]). The closeness of the fit indicates only that the refined model is a possible solution. The comprehensive review paper by Mohārir[15] on inversion of potential field data gives a detailed picture of inversion methods, covering matrix methods of inversion, estimation-theoretic inversion techniques, Backus-Gilbert inversion, regularization and use of *apriori* information, external solutions, tunneling algorithms and so on. All these procedures and algorithms attempt to relate physical models to readily observable data and determine the "best-estimates" of certain model parameters.

The problem of reconstruction of gravity anomalies due to fault lies in solving the forward and the inverse problems iteratively. In the forward modeling, the gravity anomaly is computed from a known distribution of the parameters that describe the model. This is akin to substituting values of the parameters into the equations that fully describe the model, whereas in the inverse problem, the parameters of the model are estimated from an observed gravity data set for a possible exploration of the geophysical source.

In general the exploration problems are of two types 1) the over determined and 2) the under-determined. The trivial even-determined is of rare occurrence. In all the cases a good resolution of both the model and data are desirable. The least square method solves the over-determined problem

minimising the squared Euclidean length of the error and has a perfect model resolution. Instead, the under-determined problem can be solved with a perfect data resolution by minimising the model length. In the real world, the problems are neither purely over-determined nor purely under-determined, they are mixed type. The entire field of observation over which the determination of the parameters of the model is to be carried out comes up in observation blocks some of which are over-determined while some are under-determined leading to non-uniqueness of the solution (Fisher and Howard[7], Ben-Israel and Greville[5], Ramana Murty *et al.*,[20-22], Prasanna Kumar *et al.*,[17] Torantola[17]). The generalised inverse method solves such a mixed determined problem over the whole region of observations and has both data and model resolutions intermediate between the two extremes (Penrose[16], Lancozos[11], Lawson and Hanson[12], Backus and Gilbert[2, 3 & 4]).

The generalized inverse technique, through Singular value decomposition (SVD) is an important tool (Carnhan *et al.*,[6] Ralston[23]) for the reconstruction of gravity anomalies due to a fault model. SVD is a factorisation of the operator matrix into set of orthonormal eigen vectors and associated eigenvalues. The observations are decomposed into linear combination of orthogonal eigen vectors, which in tum determine a linear combination of model parameters. Comprehensive reviews could be seen in Wiggins[28], Lanczos[11], Jackson[10], Wunsch[30] and Tarantola[27]. The advantages of SVD in construction of the Generalised Inverse Operator (GIO) are many and some of which are (1) SVD is objective and does not impose a pre-determined form to the data (2) it provides an objective means of ranking un-correlated modes of variability to determine weak signals or noise from the data and (3) it provides the modes of variability, which are not correlated with one another (Ramana Murthy *et al.*[22] Menke[14]). Further, employing SVD in GIO facilitates an explanation of the physical significance/interpretation of eigen vectors (Stidd[25], Winant *et al.*[29] and Aubray[1], Ramana Murty *et al.*[22]). These advantages of SVD led Wunsch[30] to apply GIO employing SVD in the study of ocean circulation and Roemmich[24] to compute geostropic velocity using known fields of horizontal density gradients. Further Ramana Murty *et al.*[20], Prasanna Kumar *et al.*,[17] used the SVD in Ocean Acoustic Tomography (OAT) to study the meso scale variability of ocean. In the present paper, we employ the GI technique through SVD for the reconstruction of gravity anomaly due to fault and present numerical results of Garber Oil field data (Gant and West[8]) for test validation.

2. Solution of the Inverse Problem

The model equation which relates the model (fault) to observed data expressed in the matrix from (Heiland[9], Grant and West[8], Radhakrishna Murty[18 & 19], Rao *et al.*[13]).

$$\underset{(n\times m)}{A}\ \underset{(m\times 1)}{\delta y} = \underset{(n\times 1)}{\delta z} \qquad \ldots (1)$$

where n is number of field observation points, m is number of model parameters,

$\delta z = (\delta z_i) = g_{obs}(x_i) - g_{cal}(x_i)$ is the column matrix consisting of data residual

$g_{obs}(x)$ = observed gravity value at x

$g_{cal}(x) = 2\,Gdc\,(\Pi - A)\,(Z_2 - Z_1)$ for $x = Z_1 \cot A$

and $g_{cal}(x) = 2\,Gdc\,[(x \sin A - Z_1 \cos A)\,[\sin A \ln (r_2/r_1)$

$+ \cos A\ (\phi_2 - \phi_1)] + Z_2\,\phi_2 - Z_1\,\phi_1]$, for $x \neq Z_1 \cot A$

where Z_1, Z_2 are the depths to the top and bottom of the fault, A is the fault angle, dc is the density contrast, and G is the gravitational constant.

$\delta y = (\delta y_i)$ is the column matrix consisting of model parameter perturbations

$A = (a_{ij}) = \left[\frac{\partial g_i}{\partial y_j}\right]$ is a kernel (sensitivity matrix or the matrix of partial derivatives of synthetic gravity data ($g(x_i)$) at station x_i with respect to model parameters)

i = (1, ..., n), is the station index and

j = (1, ... m), is the parameter index.

Eq. (1) is solved by SVD of the matrix A consisting of n gravity anomaly points and m model parameters expressed as a product of three matrices[11, 14 & 22]

$$\underset{(n\times m)}{A} = \underset{(n\times r)}{U}\ \underset{(r\times r)}{\Gamma}\ \underset{(r\times m)}{V^T} \qquad \ldots (2)$$

The columns of the U and V matrices are orthonormal, i.e., $U^T U = I_n$ and $V^T V = I_m$. In general, $U U^T \neq I_n$ and $V V^T \neq I_m$. U and V are the respective coupled eigen vector matrices for the eigen value problem defined as

$$(AA^T)\, u = l^2 u \qquad \ldots (3)$$

and

$$(A^T A)\, v = l^2 v \qquad \ldots (4)$$

In eq. (2) Γ is a diagonal matrix of non-zero singular values (l^2) of A, and r ($r \leq \min(n, m)$) is the rank of the matrix A.

In general, the number of model parameters in a geophysical problem is usually less than the number of field data points (gravity data points). This leads to a situation of over-determinacy, which arises when one attempts to predict the data. It would be also much easier to solve the first eigen value problem (eq. 3) than the second (eq. 4)

Once U, Γ and V obtained by solving above eigen value problems (eqs. 3 & 4), the generalised inverse solution follows as

$$\delta y_p = V V^T \delta y = (V \Gamma^{-1} U^T)\, \delta z \qquad \ldots (5)$$

If $V V^T$ equals I (if the rank of the matrix $A = m$), the solution of eq. 1 is

$$\delta y_p = \delta y = (V \Gamma^{-1} U^T)\, \delta z = (A_p^{-g})\, \delta z \qquad \ldots (6)$$

where A_p^{-g} is the natural generalised inverse operator (Jackson[10]).

If $V V^T \neq \pm$ (a case in the presence of noise in model space).

$$\delta y_p \approx \delta y = (V\Gamma^{-1} U^T)\, \delta z = (A_p^{-g})\, \delta z \qquad \ldots (7)$$

For better estimates the resolution in the model space $V V^T$ of eq. 7 is improved. This is done by judiciously selecting the p eigen vectors or ranking the singular values of the data kernel in a descending order. The noise in the data kernel (matrix A) prevailing in the form of small eigen values increases the ranking of the matrix apart from amplifying the solution. This, however, does not provide any additional or useful information on the model parameters. So, it can be treated as though the solution to the present problem is obtained through consideration of optimisation. The iteration process is continued to supplement the model parameters obtained through inversion until a reasonable fit with the observed anomaly is obtained. Such a final run is retained in memory. Once the solution is obtained, it is necessary to assess how well the data determines the model parameters. This is done through model resolution ($V_p V_p^T$) and data resolution ($U_p U_p^T$) matrices where 'p' represents the number of factors considered.

Closeness Ratio : The ratio of the sum of the factor model to that of the data matrix is considered as a measure of closeness of the model data (Ramana Murty *et al.*[21]).

$$\text{Measure of closeness} = \sum_{i=1}^{p} l_i^2 / \sum_{i=1}^{r} l_i^2 , \qquad \ldots (8)$$

where p is the number of factors considered and r is the rank of the data matrix A (Kernel). The first eigen function associated with the largest eigen value represents the broader features in the data, in the least square sense, while the second function and so on describe the residual mean square data. The closeness ratio expressed in percentage enables one to judge the contribution of different modes, and thereby reproduce the model profile. The computed eigen values and closeness ratios are presented in Table 1.

TABLE 1
Eigen values and corresponding closeness ratio for the gravity model

Sl. No.	Eigen Value	Closeness Ratio
1.	18.87	96.504
2.	2.02	2.278
3.	0.98	0.727
4.	0.73	0.280
5.	0.59	0.159
6.	0.41	0.052

3. RESULTS AND DISCUSSION

In this section computed results of a field example are discussed. SVD of kernel A (21 × 6) = $U \Gamma V^T$ has been performed using input data consisting of 21 gravity anomaly data points at 1 km

interval with amplitude ranging between 0.24-2.18 mgals taken from published work of Grant and West[8] (Fig. 2). The column matrices $U = \{u_1, u_2, \ldots, u_6\}$ and $V = \{v_1, v_2 \ldots v_6\}$ are orthonormal eigen vectors spanning data space $S(d)$, and model space $S(m)$ corresponding to eigen values Γ_i (Table 1), computed by solving eigen value problems of two covariance matrices AA^T, A^TA of 6 components contributing 100 percent of total variance. Based on the point of inflection or minimum

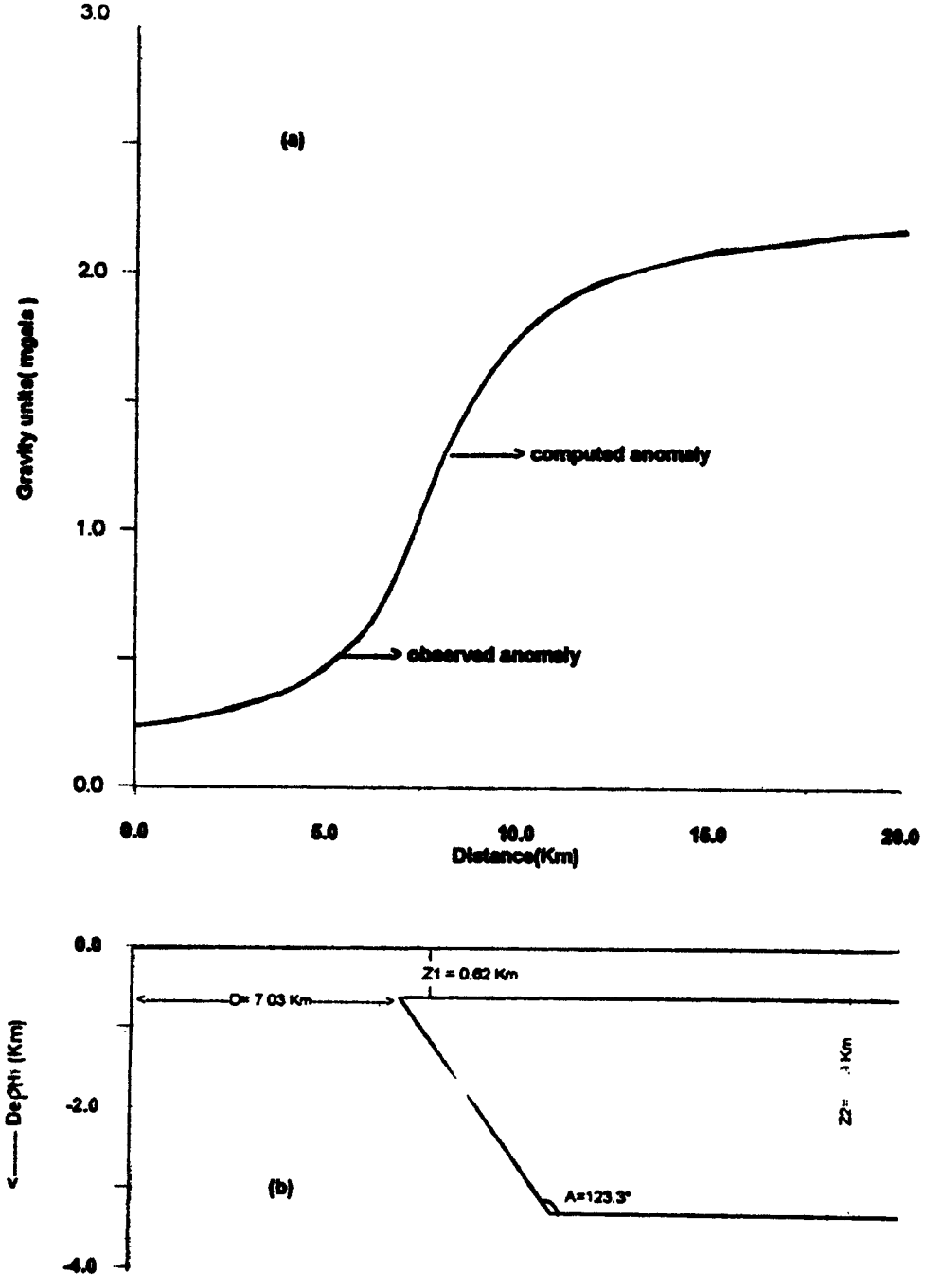

FIG. 2. (a) Observed gravity anomaly of Garber oil field and model anomaly; (b) Fault model from inversion studies

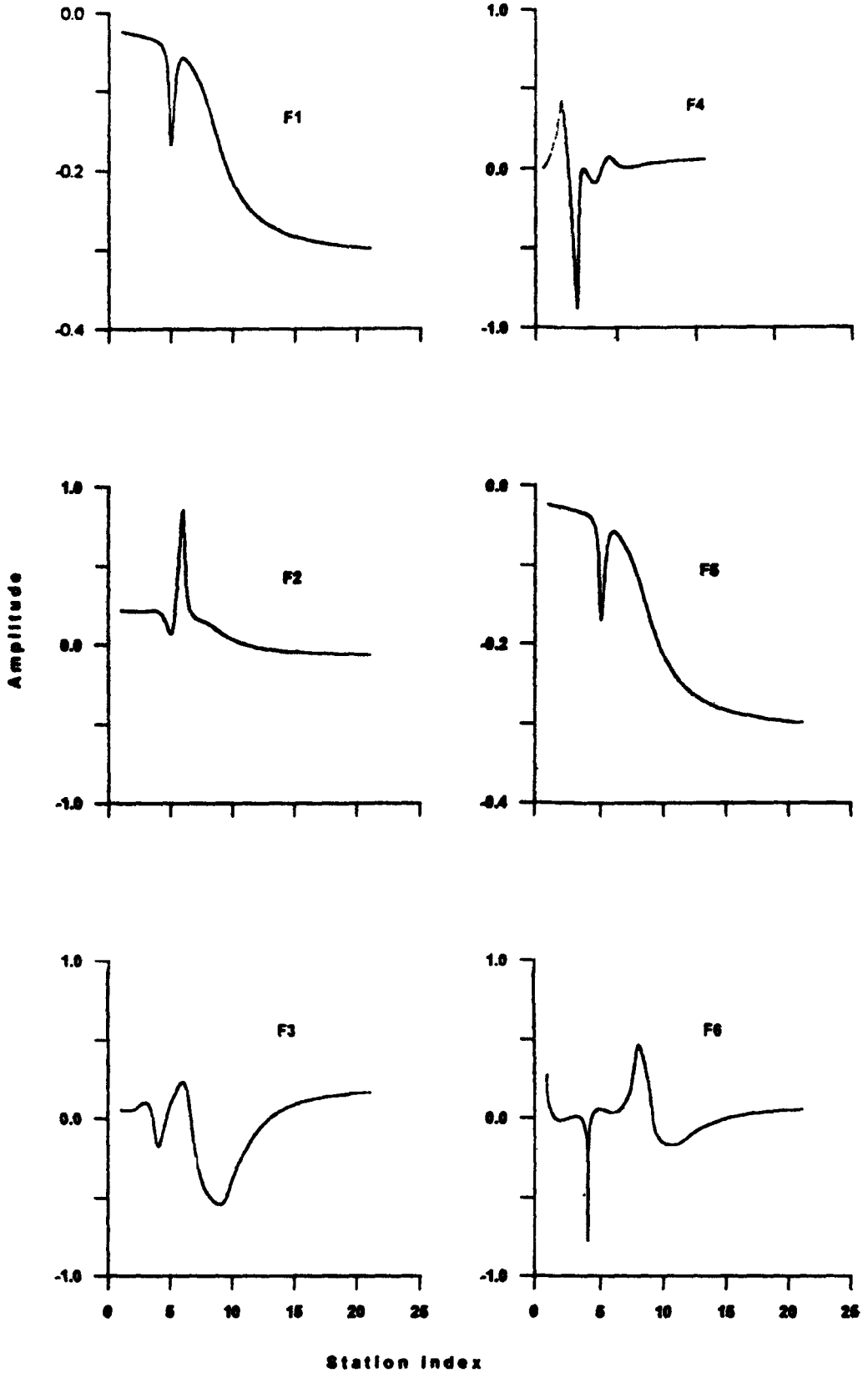

FIG. 3. Column vectors of up versus mode amplitude with varying energetic modes 1 to 6 (F1 to F6) - Garber oil field profile - over Garber oil field

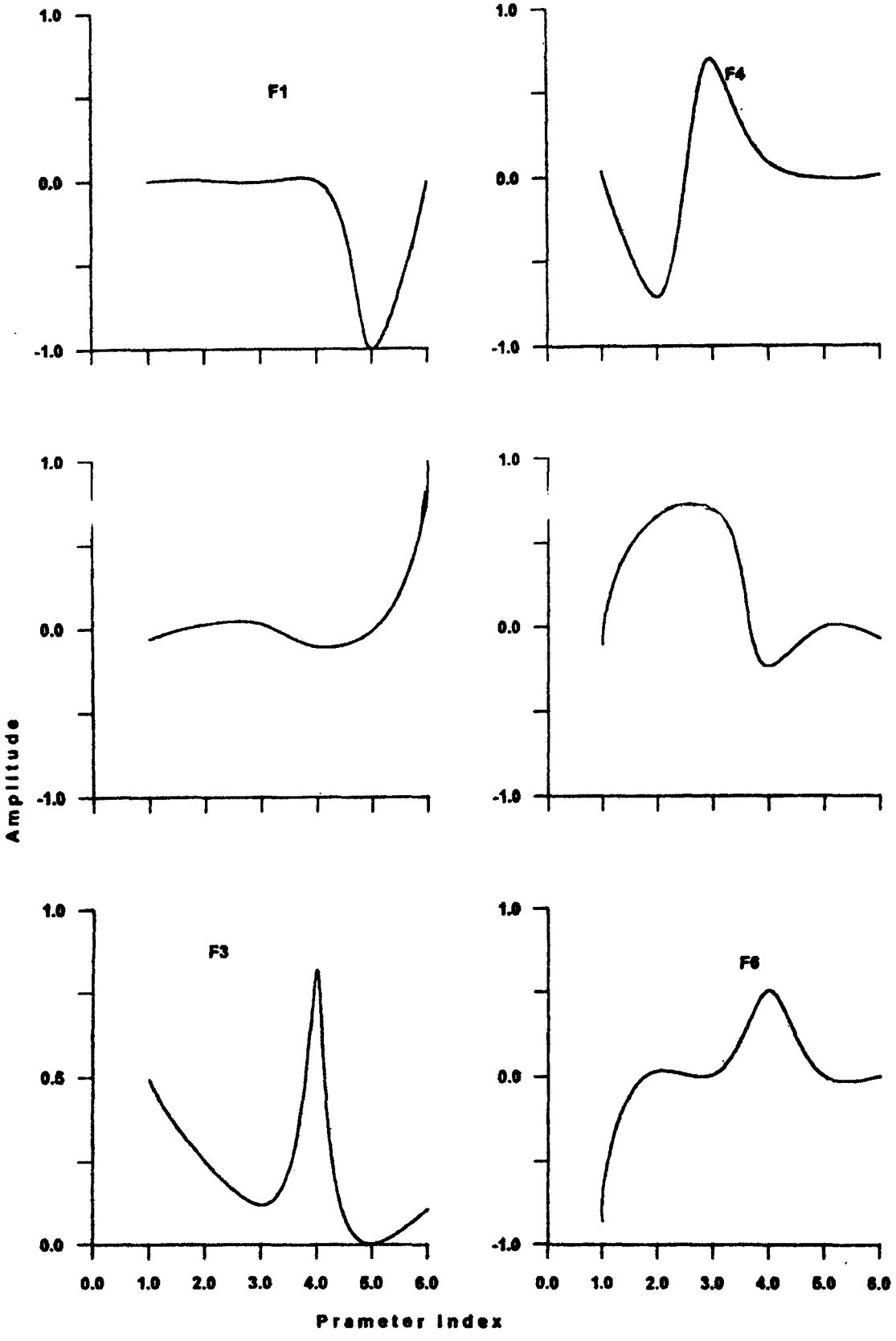

FIG. 4. Column vectors of Vp versus mode amplitude with varying energetic modes 1 to 6 (F1 to F6) profile - Garber oil field

point of cumulative eigen value two factors (p = 2) are retained for interpretation, shown in Figs. 3 & 4. The GIO $A_p^{-g} = V_p \Gamma_{-1p} U_p^T$ has been built after removing null spaces $\{U_0, V_0\}$ to operate on gravity anomaly (Fig. 2) to yield model parameters in the present numerical simulation experiment.

Using vectors in activated space, data resolution matrix $\{U_p U_p^T\}$ and model resolution matrix $\{V_p V_p^T\}$ have been computed and the elements of these matrices are presented in a contour form in (Figs. 5 & 6) respectively. The diagonal elements of model and data resolution matrices are presented respectively in tables 2 and 3. Column vectors $u_i (i = 1, \ldots 6)$ of $s(d)$ of corresponding eigenvalues of λ_i (measure of variance A in descending order) having 21 components and each component has a value indicating amplitude which explains sharing contribution of it's variance mode i. The components of u_i represents the trend or direction of spatial common features contained in kernel A ({italic partial} derivatives of gravity funmction w.r.t model parameters). Its corresponding eigenvalue λ_i represents energy level. In a similar manner the components of vectors in set $s(m)$ can be explained. The percentage contribution of individual components of $s(m)$ and $s(d)$ have been computed through closeness ratio approach (eq. 8) and shown in Tables 4 *a*, *b*. Eigen vectors derived from the data kernel of Garber oil field have been presented in Figs. 3 & 4 to explore the model and spatial parameter variability. From Figs. 3 & 4 and also from Tables 4 *a*, *b*, it can be seen

TABLE 2 :

Diagonal elements of model resolution ($V_p V_p^T$), p = 1 to 6

Parameters	Factor 1	Factor 2	Factor 3	Factor 4	Factor 5	Factor 6
Z1	0.000	0.003	0.247	0.248	0.259	1.000
Z2	0.000	0.000	0.064	0.564	0.999	1.000
A	0.000	0.001	0.015	0.505	0.999	1.000
D	0.000	0.011	0.678	0.687	0.741	1.000
Dc	0.999	0.999	0.999	1.000	1.000	1.000
DATUM	0.001	0.983	0.995	0.995	1.000	1.000

TABLE 3 :

Diagonal elements of data resolution ($U_p U_p^T$) for each station for factor p = 1 to 6

Mode No.	Number of station																				
	1	2	3	4	5	6	7	8	9	10	11	12	13	14	15	16	17	18	19	20	21
1	.001	.001	.001	.001	.282	.003	.006	.014	.030	.046	.058	.066	.072	.077	.080	.082	.084	.086	.087	.088	.089
2	.049	.047	.047	.047	.034	.730	.036	.033	.036	.047	.058	.067	.073	.078	.082	.085	.087	.089	.091	.092	.093
3	.052	.050	.057	.078	.040	.784	.076	.258	.331	.191	.102	.074	.073	.081	.090	.098	.104	.109	.114	.117	.120
4	.052	.060	.242	.082	.809	.784	.004	.258	.338	.192	.102	.074	.074	.082	.091	.100	.106	.112	.116	.120	.123
5	.052	.074	.745	.154	.884	.885	.187	.295	.350	.218	.124	.088	.081	.085	.092	.100	.106	.113	.118	.123	.127
6	.127	.074	.745	.755	.886	.886	.198	.510	.362	.243	.153	.102	.086	.086	.092	.100	.107	.114	.120	.125	.130

TABLE 4(a) :
Percentage contribution of individual components of model space s(m)

v_1%	v_2%	v_3%	v_4%	v_5%	v_6%
.095	-.055	.074	.033	-.006	-.029
.764	.025	.038	-.066	.036	.001
.668	.029	018	.065	.039	.000
.191	-.098	123	.009	-.013	.017
-95.442	-.011	000	-.001	.000	.000
-1.145	.918	016	.001	-.004	.000
98.305%	+ 1.136%	+ .269%	+ .145%	+ .098%	+ .047%

TOTAL = 100%

TABLE 4(b) :
Percentage contribution of individual components of data space s(d)

u_1%	u_2%	u_3%	u_4%	u_5%	u_6%
-.565	.092	.004	.000	.000	.005
-.661	.090	.004	.007	-.004	.000
-.759	.090	.008	.030	.022	.000
-.906	.090	-.013	-.004	.008	-.014
-4.114	.031	.006	-.061	.009	.001
-1.396	.358	.017	.000	-.010	.001
-1.910	.073	-.015	.006	.010	.002
-2.890	.058	-.035	.000	.006	.008
-4.237	.034	-.041	.005	-.003	.002
-5.241	.015	-.028	.002	-.005	-.003
-5.878	.002	-.016	.001	-.005	-.003
-6.319	-.007	-.006	.001	-.004	-.002
-6.588	-.013	.000	.002	-.003	-.001
-6.784	-.017	.004	.002	-.002	-.001
-6.931	-.019	.007	.003	-.001	-.000
-7.029	-.021	.008	.003	.000	-.000
-7.102	-.023	.010	.003	.000	.000
-7.176	-.024	.011	.004	.001	.001
-7.225	-.024	.011	.004	.001	.001
-7.274	-.026	.012	.004	.002	.001
-7.298	-.026	.012	.004	.002	.001
98.305	+ 1.135	+ .269	+ .145	+ .098	+ .047

Total = 100%

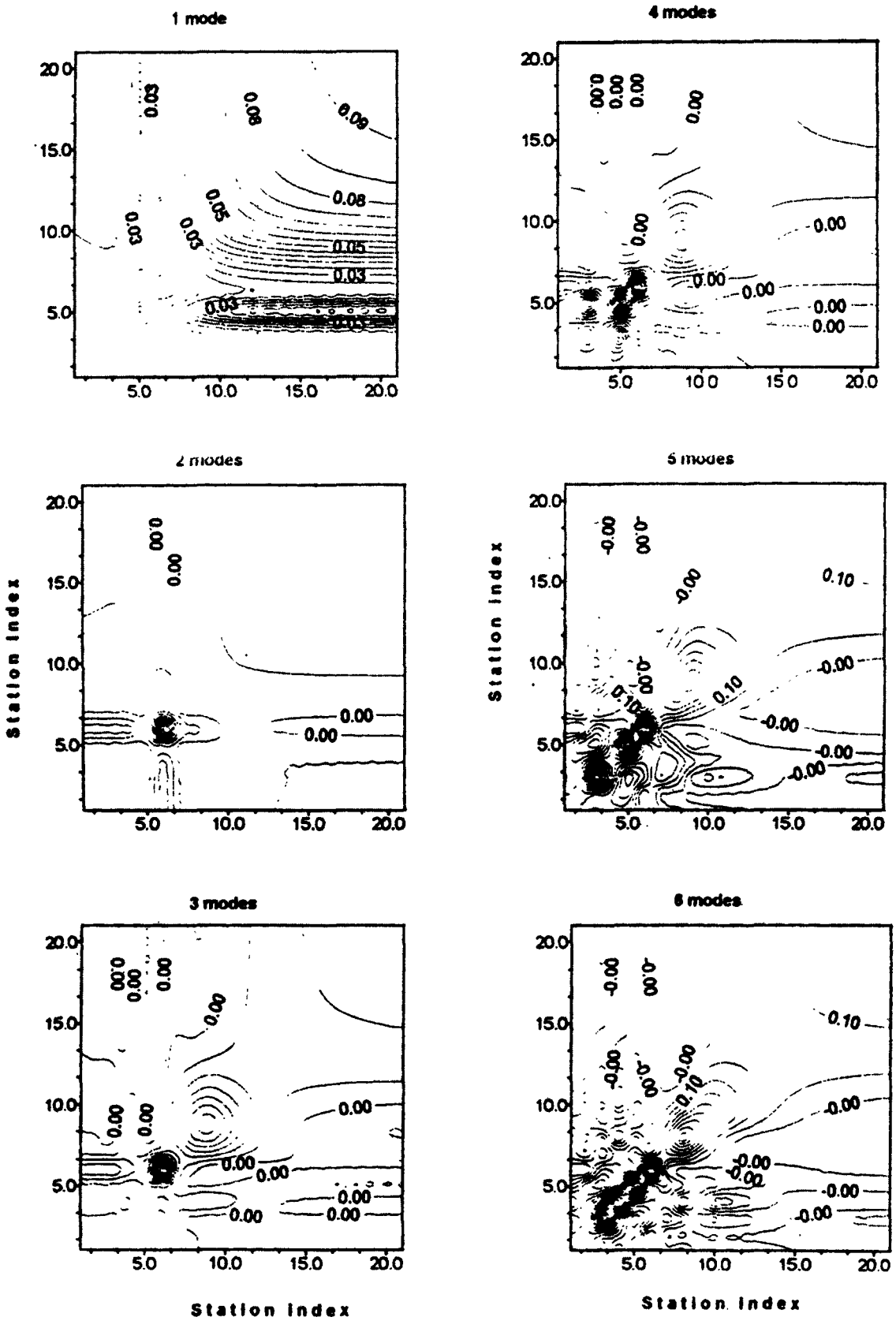

FIG. 5. 2D-Data resolution matrix (modes 1 to 6), Garber oil field

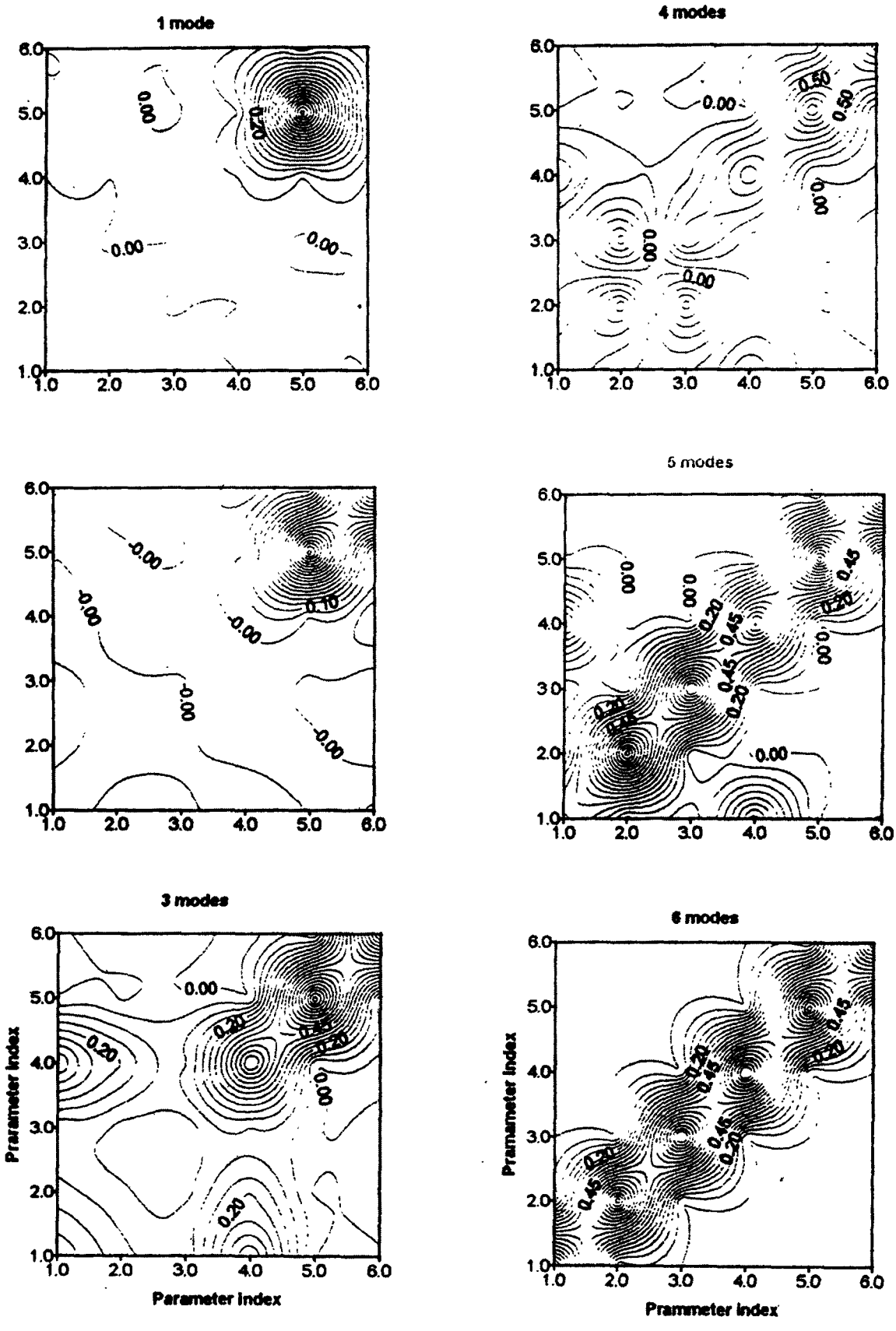

FIG. 6. 2D-Model resolution matrix (modes 1 to 6). Garber oil field

that the first two eigen functions of $s(m)$ and $s(d)$ account for more than 99% of variance predominantly represented by the first function alone. The first function u_1 in $s(d)$ and v_1 in $s(m)$ contribute 98% of total distribution representing density contrast (dc) followed by z_2 and Z_1 in that order. In general, the dc predominates to the extent of 95%. Further that, $Z_1 << Z_2$ indicates

TABLE 5 :
Gravity model analysis by natural generalised inverse approach

At the end of iteration no. 0

Distance (km)	Observed anomaly (mgals)	Calculated anomaly (mgals)	Error (mgals)
.00	.24	.24	.00
1.00	.26	.26	.00
2.00	.28	.29	-.01
3.00	.32	.33	-.01
4.00	.38	.38	.00
5.00	.48	.46	.02
6.00	.62	.60	.02
7.00	.90	.85	.05
8.00	1.28	1.34	-.06
9.00	1.56	1.64	-.08
10.00	1.76	1.80	-.04
11.00	1.88	1.89	-.01
12.00	1.96	1.96	.00
13.00	2.00	2.00	.00
14.00	2.04	2.03	.01
15.00	2.08	2.06	.02
16.00	2.09	2.08	.01
17.00	2.10	2.09	.01
18.00	2.12	2.11	.01
19.00	2.14	2.12	.02
20.00	2.16	2.12	.04

Objective function is	46.92	
Model parameters		
Depth to top of the fault is		.24km
Depth to bottom of the fault is		3.43km
Fault angle is		95.58degrees
The origin is at		7.52km
Density contrast is		.016gm/cc
Datum level is		.08mgls

At the end of iteration no. 3

Distance (km)	Observed anomaly (mgals)	Calculated anomaly (mgals)	Error (mgals)
.00	.24	.24	.00
1.00	.26	.26	.00
2.00	.28	.29	-.01
3.00	.32	.33	-.01
4.00	.38	.38	.00
5.00	.48	.47	.01
6.00	.62	.61	.01
7.00	.90	.89	.01
8.00	1.28	1.28	.00
9.00	1.56	1.56	.00
10.00	1.76	1.75	.01
11.00	1.88	1.87	.01
12.00	1.96	1.95	.01
13.00	2.00	2.00	.00
14.00	2.04	2.04	.00
15.00	2.08	2.07	.01
16.00	2.09	2.09	.00
17.00	2.10	2.11	-.01
18.00	2.12	2.13	-.01
19.00	2.14	2.14	.00
20.00	2.16	2.15	.01

Objective function is .00

Model parameters

Depth to top of the fault is	.62km
Depth to bottom of the fault is	3.29km
Fault angle is	123.27°
The origin is at	7.03km
Density contrast is	.020gm/cc
Datum level is	.07mgals

that the fault is thin in nature from the location of 12^{th} station onwards to the end (Table 4 *a*, *b*). The contribution of remaining functions in $s(d)$ and $s(m)$ is only 1.7% of total information, too insignificant to consider for interpretation.

The first two energetic spatial and model functions of $s(d)$ & $s(m)$ have been used to bring the predictale rich part of the original signal to obtain inverse solution (Fig. 2 and Table 5) by

operating GIO on gravity anomaly and for construction of data and model resolution matrices (Figs. 5 & 6). The results obtained from GIO analysis of gravity anomaly of Garber oil field indicate that the thickness $(Z_2 - Z_1)$ of fault is 2.67 km with density contrast of 0.02gm/cc and fault angle (A) 123° (table 5) with the fault origin (D) located at 7.03 km. from the reference point (Fig. 1). It can be seen from Fig. 2 that the gravity anomaly computed using the model and the anomaly observed match exactly validating the present procedure.

Data Resolution : The data resolution matrix is an indication of the information density of the data kernel i.e., it indiates which data contribute independent information to the solution. The diagonal elements of $U\,U^T$ are shown in Table 3, for factors 1, 2... 6. A value of unity for any particular parameter shows that the influence of the respective parameter dominates that of all the other parameters describing the model. Table 3 enables one to infer which of the data points present strong/poor information resolution. The data resolution is given by,

$$N = AA_p^{-g} = U_p\,U_p^T.$$

The data are perfectly resolved if U_p spans the complete space of data. The small eigen values in the data kernel (Matrix A) increases the rank of the matrix (i.e., the dimension of the activated space) besides amplifying the solution due to the presence of noise. In this case one should not consider the eigen vectors corresponding to small eigen values (< 1). If we consider the eigen vectors corresponding to very small eigen values, while estimating the solution, then it is very likely that high frequency noise components predominate the inverse estimates masking the original signal. Fig. 5 (mode 1) describes the contour map of the resolution matrix $u_1\,u_1^T$ where u_1 is the highest spatial energetic mode of $s\,(d)$. It gives 98.305% variance of the total information i.e., mostly gross features of the kernel (Table 1). The resolution is seen to increase gradually from the first station to 5th station. Afterwards the data resolution is high between stations 5 to 21 indicating discontinuity in density. This fact is confirmed by first vector of $s\,(d)$ (Figs. 5 & 6, mode 1 and Table 2). The remaining 5 eigen functions (modes 2 to 6) contribute < 2% information and can be treated as noise and neglected for interpretation.

Model Resolution : The model resolution of the Generalised inverse is given by $R = A_p^{-g}\,A = V_p\,V_p^T$,. Here p indicates number of factors used in SVD, which is less than or equal to the rank of matrix A. The model parameters will be perfectly resolved if V_p spans the complete space of the model parameters, i.e. $V_p\,V_p^T = I$. The model resolution is perfect for the contribution of gravity anomaly due to the density contrast (shown in Fig. 6, mode 1 and Table 2) and one can conclude that density is independent of other model parameters and it is of homogeneous nature. This is also reflected in the data resolution (Fig. 5, mode 1) between stations 5-20 (and Table 3).

The present study indicates that the partial information contained in the data space is adequate to reconstruct the model parameters. This reveals the usefulness of natural generalised inverse in the least square sense in handling problems of over determinacy.

4. CONCLUSIONS

I. SVD analysis carried out on Garber oil field data, Oklahoma, shows that the first two energetic modes of data space $s(d)$ and model space $s(m)$ contribute 99.3% to the total distribution, (density contrast 98% and datum level : < 2%).

II. A good agreement has been found between the predicted model anomaly and the observed gravity anomaly.

III. Inverse solution reveals that fault model parameters are : depth to top of the fault: 0.62 km; depth to bottom of the fault: 3.29 km; fault angle: 123.27°, origin : 7.03 km; density contrast: 0.020gm/cc and datum level:0.07mgals which agree quite well with the known results.

ACKNOWLEDGEMENTS

The authors are thankful to Dr. E. Desa, Director, National Institute of Oceanography, for his constant encouragement and keen interest in this study. Thanks are also due to Mr. Ch. Jawahar Kumar, Mr. S. Ramesh for their secretarial assistance in preparation of this paper. They take pleasure in thanking the anonymous referee whose meticulous criticism helped to improve the quality of presentation. This is NIO contributions No. 37671.

REFERENCES

1. D. G. Aubray, *Ph. D. Dissert.* 1978, p 194, Scripts Institute of Oceanography, San Diego, Calf.
2. G. E. Backus and J. F. Gilbert, *Geophys. J. astron. Soc.* **13** (1967) 247-76.
3. G. E. Backus and J. F. Gilbert, *Geophys. J. astron. Soc.***16** (1968) 169-205.
4. G. E. Backus and J. F. Gilbert, *Phil. Trans. Roy. Soc., London, Ser A* **266** (1970) 123-92.
5. A. Ben-Israel and T. N. E. *Greville, Generalised Inverses: Theory and Applications*, John Wiley and Sons, Inc. pp 395, 1974.
6. B. Camhan, H. A. Luther and J. O. Wilkes, *Applied Numerical Methods*, John Wiley, New York p 604 1969.
7. N. J. Fisher and L. E. Howard, *Geophysics*, **45** (1980), 403-15.
8. F. S. Grant and G. F. West, *Interpretation Theory in Applied Geophysics*, McGraw Hill Co., New York, p. 584, 1965.
9. C. A. Heiland, *Geophysical Exploration*, hanfer Publishing Company, New york, p 150-53, 1963.
10. D. D. Jackson, *Geophys.. astron. Soc.*, **28** 97-109, 1972.
11. C. Lanczos, *Linear Differential Operators*, Princeton: D Van Nostrand, 1961.
12. Ch. L. Lawson and R. J. Hanson, *Solving Least Squares Problems*, Prentice Hall, 1974.
13. M. Malleswara Rao, S. Lakshminarayana, A. S. Subramanyam, K. S. R. Murthy, Comp. Geoscie. **19**, No. 5 657-72, 1993.
14. W. Menke, *Geophysical Data Analysis: Discrete Inverse Theory*, Academic press, New York p 260, 1984.
15. P. S. Moharir, *Proc. Indian Acad. Sci. (Earth Planet. Sci.)*, **99**, No. 4, (1990) 473-514.
16. R. Penrose, *Proc. Camb. phil. Soc.* **51** (1955) 401-13.
17. S. Prasanna Kumar, G. S. Navelkar, T. V. Ramana Murthy and C. S. Murthy, *Acoustica* **83** (1997) 847-54.
18. I. V. Radhakrishna Murthy and S. K. G. krishnamacharyulu, *Comput. Geosci.* **16**(4) (1990) 539-48.

19. I. V. Radhakrishna Murthy, Gravity and Magnetic interpretations in *Explorations Geophysic, Mem. geology Soc. India* No. **40** (1998) p 363.
20. T. V. Ramana Murthy, Y. K. Somayajulu and C. S. Murthy, *Indian J. marine Sci.* **25** (1998) 328-34.
21. T. V. Ramana Murthy, Y. K. Somayajulu, R. Mahadevan, C. S. Murthy, C. S. and J.S. Sastry. *Defence Sci. J.* **42** (1992) No. 2, 89-101.
22. T. V. Ramana Murthy, M. Veerayya and C. S. Murty, *Sediment-size distributions of the beach and nearshore environs* along the central west coast of India: an analysis using EOF, J. Geophys. Re., **91** (C7), (1986) p 8523-26.
23. A. Ralston, (*Ed.*), *Mathematical Methods for Digital Computers*, John Wiley, New York p. 293 1966.
24. D. Roemmich, *J. Geophys. Res.*, **86** (1981) Bi (C9), 7993-8005.
25. C. K. Stidd, *J. appl. Meterol.* **2** (1967) 255-64.
26. M. Talwani and J. Heirtizler, *In*: *Computers in Mineral Industries*, Part 1, *Stanford univ. Publ. Geol. Sci.*, **9** (1964) 464-80.
27. A. Tarantola, *Inverse Problem Theory: Methods for Data Fitting and Model Parameter Estimation*, Elsevier, Amsterdam p 613, 1987.
28. R. A. Wiggins, Rev. Geophysics and space physics, **10** (1972), 251-85.
29. C. D. Winant,D. L. Inman and C. E. Nordstam, *J. Geophys. Res.* **80** (15) (1975) 1979-86.
30. C. Wunsch, *Tracer Inverse Problems in Oceanic Circulation Models: Combining Data and Dynamics* (*Eds.* D. L. T. Anderson and J. Willebrand.) Kluwer Academic Publishers, Hingham, p. 1-77, 1989.